IEEE Access
Multidisciplinary ⋮ Rapid Review ⋮ Open Access Journal

Received February 11, 2019, accepted February 28, 2019, date of publication March 11, 2019, date of current version March 29, 2019.

Digital Object Identifier 10.1109/ACCESS.2019.2904201

Empirical Based Ranging Error Mitigation in IR-UWB: A Fuzzy Approach

SUNIL K. MEGHANI[1], MUHAMMAD ASIF[2], FAROQ AWIN[1,3], AND KEMAL TEPE[1]

[1]WiCIP Lab, University of Windsor, Windsor, ON N9G 3B2, Canada
[2]Electrical Engineering Department, Faculty of Engineering Science and Technology, Ziauddin University, Karachi 74600, Pakistan
[3]Electrical and Electronic Engineering Department, Faculty of Engineering, University of Tripoli, Tripoli 13555, Libya

Corresponding author: Sunil K. Meghani (kumar11d@uwindsor.ca)

ABSTRACT Indoor tracking and navigation (ITN) mainly depend on indoor localization. An impulse radio ultra-wideband (IR-UWB) is the most advanced technology for precision indoor localization. Besides its precision, the IR-UWB also has low complex hardware, low power consumption, and a flexible data rate that makes it the ideal candidate for ITN. However, two significant challenges impede the achievement of high-resolution accuracy and optimum performance: non-line-of-sight (NLOS) channel condition and multipath propagation (MPP). To enhance the performance under these conditions, the ranging error is estimated and corrected using parameters' uncertainties. The uncertainties in the channel's parameters have a relationship with the error, and these uncertainties are induced due to the NLOS and MPP propagation conditions. The parameters are collected in real-time experimental setups in two different environments. A proposed fuzzy inference model utilizes these uncertainties and the relationship to estimate ranging errors. The model is evaluated, and its performance is gauged in terms of residual ranging error cumulative distribution, root mean square error, and outage probability parameters using experimental measurements and compared with the state-of-the-art work. Moreover, the proposed fuzzy model is evaluated for computational complexity in terms of execution time and compared with the state-of-the-art work. The time is estimated on the targeted embedded system. The experimental and simulated results show that the proposed model effectively minimizes the ranging errors and computational burden. Moreover, the model does not induce a delay in estimating ranging error due to the non-statistical based solution.

INDEX TERMS Fuzzy logic, indoor tracking and navigation, impulse radio ultrawide band, localization, computational complexity.

I. INTRODUCTION

In recent years, indoor tracking and navigation (ITN) system has been attracting the attention of the research community due to the proliferation of unmanned vehicles and drones within civilian and military applications [1], [2]. ITN also enhances the functionality and expands the capabilities of applications in mobile wireless sensor networks, infrastructure monitoring, healthcare, mining, and military domains [2]–[4]. Legacy Global Navigation Satellite System (GNSS) provides a satisfactory performance that supports tracking and navigation in open space. However, the performance of GNSS depends on the reception of satellite signals [1], [2]. In the case of the indoor environment, the reception of the signals is so weak, which significantly inhibits GNSS performance [2]. Moreover, inertial measurement unit (IMU) sensors support dead reckoning based tracking and navigation [4], [5]. However, the IMU sensors-based tracking and navigation alone is not suitable for precise ITN [5]. Therefore, there are wireless standards that enable and support ITN due to enabled localization feature, such as Wi-Fi, Bluetooth, ZigBee, Impulse Radio Ultra-Wideband (IR-UWB), and radio frequency identification RFID [3], [6]–[8]. Among those standards, IR-UWB is the leading technology for providing high-resolution localization [9]–[11]. Besides precision ranging, IR-UWB's salient features include through-wall propagation, low power consumption, and size form factor bode well for mobile devices [9]–[13]. However, multipath propagation (MPP) and non-line-of-sight (NLOS) conditions, which frequently occur in indoor environments, are impeding in the achievement of sub-centimeter resolution and degrading the performance of ITN systems [7], [11], [13]. There are limited existing studies [11], [14]–[21] which provide

The associate editor coordinating the review of this manuscript and approving it for publication was Giovanni Pau.

solutions to mitigate ranging errors. A comprehensive review of those studies is provided in Section II. However, due to limited computational resources of mobile devices and ITN's stringent delay requirement, those studies have some deficiencies which are as follows:

- The range statistical based solutions induce delay.
- The CIR parametric statistical based solutions induce delay.
- The machine learning based solutions are cumbersome to implement on a real-time embedded system due to limited computational resources. Furthermore, machine learning methodology requires mandatory training phase which incurs an extra overhead (i.e., time and memory).
- The full-length channel impulse response (CIR) data based Fuzzy model slows down the ranging procedure and adds latency [22].

Those deficiencies motivated us to propose a fuzzy logic-based model to estimate and correct the range bias error; since such a non-statistical approach aligns with the strict bound on computational complexity and ranging acquisition delay. Moreover, the uncertainties in the measurements, which are induced due to MPP and NLOS, are covered optimally by the fuzzy approach. The range bias error is estimated in one step rather than in two steps (i.e., first, identification of line-of-sight (LOS)/NLOS; second, mitigation of ranging errors). We start by analyzing the uncertainties in the CIR's parameters (i.e., received power, received first path power and rise time). Then, we propose a fuzzy inference system (FIS) based model which is based on the uncertainties in the parameters and their correlation to ranging error. In addition to NLOS errors, we consider the error in LOS conditions due to MPP in the proposed model. Finally, we evaluate the proposed model using real-time experimental data in two different environments and compare the ranging error mitigation performance with the existing fuzzy logic-based obstruction identification and mitigation method [14] and machine learning methods for error mitigation [18]. In addition, the proposed model is evaluated and compared with the works mentioned above (i.e., [14] and [18]) in terms of computational time. The time is a key parameter for computational complexity estimation and system resources utilization [23], [24]. The main contribution of this work is to propose a range error mitigation model using the fuzzy logic approach with parameters that do not incur a delay in estimating and correcting the errors and reduced computational complexity in IR-UWB domain. To the best of authors' knowledge, the approach was not employed in the domain.

The rest of the paper is organized as follows: Section II presents a comprehensive review of the existing work. Section III defines the problem statement. Section IV presents the uncertainties analysis, concerning the severity of the NLOS condition and MPP in LOS condition in the CIR's parameters and their relationship with ranging errors. The detailed proposed FIS model is presented in Section V. Experimental setups and scenarios are presented in Section VI. Localization performance evaluation is discussed in Section VII. Finally, the conclusion is drawn in Section VII.

II. LITERATURE REVIEW

The current literature includes some studies that provide solutions to mitigate ranging errors bias due to NLOS conditions within the IR-UWB domain. The mitigation solutions are mainly based on better detection of edges (i.e., leading edge detection algorithm) and system level soft computing CIR parametric approach [11], [14]–[21]. The parametric mitigation methodology is mostly based on five key factors: range statistics, CIR parameters' statistics, CIR parameters' energy (or power) levels, machine learning methods based on waveforms' (or CIR) parameters, and fuzzy-based model for obstruction detection. Yousefi *et al.* [15] propose derivation of weights from range statistics. The weights are proportional to the severity of NLOS conditions and utilize in an extended Kalman filter (EKF) for correcting the position estimation in NLOS conditions. However, estimating range variation for a moving target is not feasible particularly in NLOS conditions and introduces latency in range estimation [17]. The CIR parameters' statistics-based identification of LOS/NLOS and mitigation of range error bias in NLOS conditions study in [16]. The parameters' statistics for this technique are based on kurtosis and mean root mean square (RMS) delay. The technique identifies the LOS/NLOS conditions and mitigates the range error in NLOS conditions based on the derivation of weights that are related to the severity of the NLOS conditions. Moreover, the proposed technique has been evaluated based on simulated 802.15.4a (IEEE standard for IR-UWB) channel models. Besides, Silva and Hancke [11] employ a similar technique to [16]; however, they assess their technique using real-time measurements in an industrial environment for the identification of LOS/NLOS conditions.

On the other hand, the CIR parametric statistic technique also introduces latency, since it is a statistical-based solution. Marano *et al.* [17] propose least square support vector machine (LS-SVM), a machine learning based model, to identify the LOS/NLOS conditions and to mitigate the ranging error bias in NLOS conditions. The authors evaluate the performance of their model using real-time experimental data. Moreover, Wymeersch *et al.* [18] suggest range errors bias mitigation technique as a one-step procedure using machine learning methodology (i.e., directly estimating ranging error) instead of performing two-steps procedure (i.e., identification of LOS/NLOS and range error mitigation) which increases the complexity. The technique uses two machine learning methods (i.e., SVM and gaussian regressions) and the residual ranging error is used to evaluate the technique's performance. Furthermore, the work in [19] proposes to employ a support vector data description (SVDD) machine learning based regression methodology for ranging error mitigation, which is also a one-step procedure. The work analyzes the percentage of training data and its impact on the ranging error mitigation accuracy.

The above-mentioned machine learning-based techniques were employed to identify the NLOS conditions and to mitigate the range error bias; however, they are not feasible in a practical real-time system because they dramatically incur a computational complexity [20]. Moreover, machine learning based methods are time-consuming due to the mandatory training phases and highly dependent on the uncertainties of the environments. In [20], after the identification phase, the authors have derived weights for the severity of the NLOS conditions based on statistics of propagation time compared to LOS time of flight (ToF). You *et al.* [21] empirically identify the LOS/NLOS conditions based on first path power (or energy) and overall received power.

The FIS based classification has been studied in general and particularly in a wireless system and positioning for various problems [14], [25], [26]. Wen *et al.* [14] purpose obstruction identification based NLOS range error mitigation based on a fuzzy mapping between signal characteristics (inputs) and likely obstruction (output). There are four signal characteristics: signal-to-noise ratio (SNR), RMS delay spread, kurtosis and skewness for identification of predefined obstructions (propagations). After identification of LOS/NLOS conditions, the range error is compensated using a predefined range error for the obstruction. The authors validate and evaluate their empirical fuzzy logic model in predefined propagation scenarios. On the other hand, the CIR frame length data is required for estimating the signal characteristics. However, acquiring the CIR frame length data in runtime slows down the ranging process, and adds a delay in estimating range between anchor and agent nodes [22].

III. PROBLEM STATEMENT

In this section, ranging errors that inhibit localization performance are discussed. First, the localization procedure and the algorithm are described. Second, the source of ranging errors and its impact are considered.

A. AGENT LOCALIZATION

In the localization network, nodes are classified as an anchor or an agent. An anchor is a node with the known position while an agent is a node with the unknown position. A typical single node localization requires three or more anchor nodes as well as a single agent node whose position needs to be determined. To describe a scenario, let an agent be at an unknown position denoted by P. The agent is surrounded by N_a anchor nodes with known positions denoted by A_i, where $i = 1, 2, \ldots N_a$ and N_a is the maximum number of anchors. The coordinates of the agent and the anchors are labelled as (x_P, y_P) and (x_{A_i}, y_{A_i}) for 2-dimensional (2D) space or (x_P, y_P, z_P) and $(x_{A_i}, y_{A_i}, z_{A_i})$ for 3-dimensional (3D) space respectively. The true distance between the agent and the i^{th} anchor is given by $d_i = \|P - A_i\|$.

To localize the agent, the distances between the agent and the anchors within the vicinity need to be estimated, using the ranging algorithm. Let $\hat{d}_i$ be the estimated distance between the i^{th} anchor and the agent. In the 2D space, using position algorithm, minimum three estimated distances are required to determine the agent position. A typical solution to this problem is to use the least square (LS) algorithm, which is provided by:

$$\hat{P} = arg_T^{min} \sum_{\left(A_i, \hat{d}_i\right) \in O} \left(\hat{d}_i - \|T - Ai\|\right)^2 \tag{1}$$

where O is the number of agent-anchor pairs in the vicinity. For the 2D space, minimum $O = 3$. The agent can estimate its position by minimizing (1), which is determined numerically by solving (1) using linearization methods such as pseudo inverse [27]. However, LS algorithm does not consider ranging errors.

B. RANGING ERROR

In practice, the ranging errors are introduced by a ranging protocol, MPP and NLOS channel conditions between an agent and anchors. The NLOS channel condition induces a significant ranging error mainly due to obstructions between anchor and agent nodes which results in position errors when using (1) to estimate a position. The ranging errors are induced by either an attenuated first path or a complete blockage of the first path because of having obstructions. Moreover, in NLOS condition, overall received power is attenuated compared to LOS condition. The ranging error is given by $\varepsilon_i = \hat{d}_i - d_i$. Based on our experimental studies, we note the following observations:

1. The ranging errors in LOS and NLOS conditions are exhibit differently. In case of LOS, the ranging errors are confined to 10 cm. However, in NLOS conditions, the ranging errors are expanded up to 110 cm.
2. The enabling of full-length CIR data slows down the ranging process.
3. Collecting multiple ranges increases acquisition time.
4. Implementing machine learning methods increases computational complexity.

Therefore, to reduce the errors along with a reduction in computational complexity and an improvement in the localization performance, we propose a non-statistical based FIS based model to mitigate ranging errors.

IV. PARAMETERS UNCERTAINTIES

In this section, the uncertainties in the CIR parameters are considered, and the relationship between parameters' uncertainties and ranging errors is defined. The relationship is employed as expert-based knowledge for the proposed FIS model. In general, the uncertainties may occur due to LOS/NLOS conditions, multipath, measurement noise, and unknown dynamics. However, most of those uncertainties are induced by NLOS conditions. The uncertainties can be lumped into one single block Δ.

Considering the uncertainties, the CIR measurement model can be partitioned into a nominal part and an uncertain

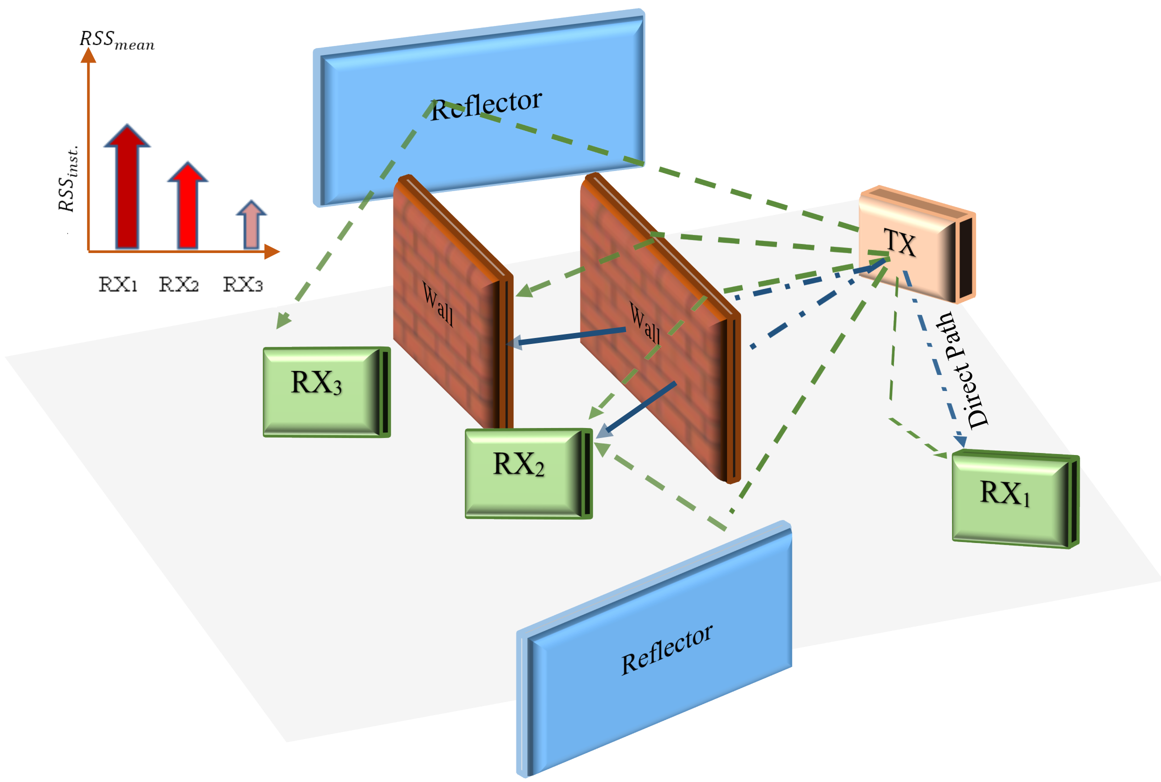

FIGURE 1. Relationship between the received signal strength (RSS) and line-of-sight (LOS) or non-line-of-sight (NLOS) condition.

part as:

$$CIR(t) = CIR_N(t) + CIR_\Delta(t) \tag{2}$$

where $CIR_N(t)$ is the nominal value and $CIR_\Delta(t)$ is the uncertain part and satisfy the condition $CIR_\Delta(t) \le \eta, \forall t \ge 0$, where η is a positive variable [28]. This measurement model enables relaxing to determine the requirement of exact knowledge of $CIR(t)$ and uncertainties and their correlation to range error at any given instant. The CIR parameters: received signal strength (RSS), first path power strength (FPPS) and rise time (RT).

A. RECEIVED SIGNAL STRENGTH (RSS)

There is a correlation between RSS, transmitted power, and the distance between transmitter and receiver as computed using the Friis equation [29]. The RSS estimated using the equation is labeled as RSS_{mean}. In addition, RSS is affected by multipath propagation components (MPCs) and condition of the channel (LOS or NLOS) as illustrated in Fig. 1 For the scenario illustrated in Fig. 1, it is assumed that three receivers (RXs) are placed at equidistance from the transmitter (TX). The RX_1 received instantaneous power close to RSS_{mean} power level while power levels received by RX_2 and RX_3 are attenuated due to NLOS conditions. The RX_3 power is primarily attenuated by multiple obstructions and RX_3 is categorized as in severe NLOS condition. The instantaneous RSS varies due to MPCs, and the LOS/NLOS condition can be modeled as follows:

$$RSS_{inst.} = \begin{cases} RSS_{mean} + L & N = 0(LOS) \\ RSS_{mean} + L + N & N < 0(NLOS) \end{cases} \tag{3}$$

where L is the MPP factor in dBs and N is the attenuation factor due to NLOS conditions in dBs. The constants (i.e., L and N) show uncertainties induced due to MPP and NLOS conditions, respectively. Note that N is proportional to the severity of NLOS conditions. For less severe NLOS condition, N is low and causes less uncertainty in RSS_{mean} magnitude. However, for severe NLOS condition, N is high and more RSS_{mean} is attenuated. For the LOS condition, $RSS_{inst.}$ is close to RSS_{mean} and MPP induces a very low uncertainty. The $RSS_{inst.}$ is estimated in Decawave devices using received CIR magnitudes [22].

B. FIRST PATH POWER STRENGTH (FPPS)

In IR-UWB, the FPPS (instantaneous) is estimated using CIR leading edge MPC (F_1) followed by two MPCs in CIR (F_2 and F_3) [22] as illustrated in Fig. 2. For ranging estimation, leading edge detection (LED) algorithm is employed to detect F_1 based on time of arrival (ToA) technique. Therefore, detection of FPPS is vital for correct ranging estimation in IR-UWB. Like $RSS_{inst.}$, instantaneous FPPS varies due to MPCs and the channel condition. Therefore, the FPPS can be modelled as follows:

$$FPPS_{inst} = \begin{cases} FPPS_{mean} + L_{FP} & N_{FP} = 0\,(LOS) \\ FPPS_{mean} + L_{FP} + N_{FP} & N_{FP} < 0(NLOS) \end{cases} \tag{4}$$

where L_{FP} is the MPP factor in dB and N_{FP} is the first path NLOS attenuation factor in dB. The magnitude of N_{FP} depends on the obstruction material and the number of obstructions in NLOS conditions. As $RSS_{inst.}$ and $FPPS_{inst.}$ are estimated using CIR magnitude. Hence, they are correlated with each other.

C. RISE TIME (RT)

RT is defined as the difference between the time occurrence of F_1, denoted as T_{F_1}, and time occurrence of maximum MPC (F_{max}), denoted as $T_{F_{max}}$, and can be modeled as:

$$RT = T_{F_{max}} - T_{F_1} \tag{5}$$

RT varies according to the condition as demonstrated in Fig. 2. The figure shows that RT, in LOS condition, is low while it is high in NLOS condition respectively. The RT magnitude also depends on the severity of NLOS.

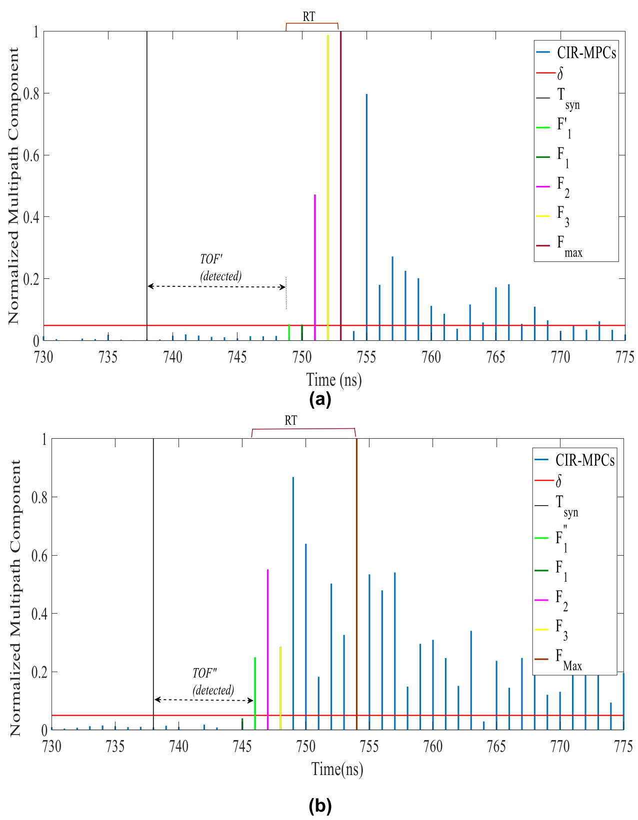

FIGURE 2. Channel impulse responses. (a) LOS. (b) NLOS.

D. RANGING ERROR AND FPPS

For the LED algorithm, the first MPC above the threshold is considered as the first path. Based on that, the distance between the TX and the RX is estimated as:

$$TOF = T_{F_1} - T_{syn} \tag{6}$$

$$\hat{d} = TOF.C \tag{7}$$

where C is the speed of light; TOF is the time of flight; T_{syn} is the time at which TX and RX are synchronized; and T_{F_1} is the time at which F_1 (leading edge magnitude) detected, provided:

$$F_1 > \delta \tag{8}$$

where δ is the threshold level for ToA based estimator (i.e., the receiver). However, F_1 depends on the received power and the channel condition as provided in (4). In addition, the ranging error depends on detection scenarios of F_1, such as early detection and post detection.

Case I (Early Detection): This case is commonly observed in LOS conditions due to MPP. Assume that the leading edge is detected earlier than the true F_1, as shown in Fig. 2(a), (i.e., $F_{1'}$). The new time-of-flight (i.e., TOF') is computed as:

$$TOF^{'} = T_{F_{1'}} - T_{syn} \tag{9}$$

such that:

$$T_{F_{1'}} < T_{F_1} \tag{10}$$

$$\Delta T = T_{F_{1'}} - T_{F_1} \tag{11}$$

Error in the distance is given by:

$$e = \Delta T.C \tag{12}$$

From (11), the estimated distance is shorter than the true distance and the ranging error is negative. From (3), (4) and (12), the ranging error depends on the $RSS_{inst.}$ and $FPPS_{inst.}$ power levels in LOS conditions.

Case II (Post Detection): It is the case where an NLOS condition is present. In this case, the leading edge is detected after the true F_1, as shown in Fig. 2(b), (i.e., F_1''). The time-of-flight, TOF'', is estimated using (6). However,

$$T_{F_1''} > T_{F_1} \tag{13}$$

using (11), ΔT is positive. Hence, the error is positive, thus, the error magnitude is correlated with the received $RSS_{inst.}$ and $FPPS_{inst.}$ magnitudes. Further, the magnitudes of $RSS_{inst.}$ and $FPPS_{inst.}$ are related to NLOS severity as in (3) and (4).

V. FUZZY INFERENCE SYSTEM (FIS) MODEL

The parameters' uncertainties and their correlation to the ranging error are indicators to the channel condition (i.e., LOS or NLOS) and the severity of the NLOS condition, as shown in the preceding section. To overcome the ranging error due to these uncertainties, the FIS model is presented in this section.

There are three types of FIS: Mamdani, Surgeno, and Takagi–Sugeno–Kang (TSK) [30]. However, Mamdani FIS is widely used for its analogy to human interpretation and easiness of design [30]. In this work, we employ the Mamdani

FIS for estimating ranging error. The particular Mamdani multiple input single output (MISO) FIS can be written as follows:

$$\varphi(r_i) = \beta(r_i) + y, \tag{14}$$

where φ is the fuzzified weight of a particular rule r_i, $\beta(r_i)$ is the firing strength of the rule, and y is the area of the consequent membership function (MF) of r_i.

$$Z = \frac{\int \mu_Y(y)\, y dy}{\int \mu_Y(y)\, dy}, \tag{15}$$

where $\mu_Y(y)$ is the output membership function (MF) of output y.

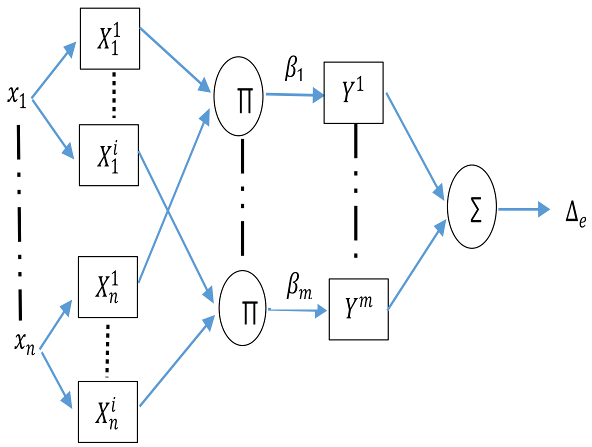

FIGURE 3. Fuzzy inference system model.

The employed Mamdani MISO FIS model is depicted in Fig. 3. From the figure, n is the number of inputs, $n \in \{1, 2, 3\}$, i is the total number of MFs, and m is the number of rules, while X_n^i and Y^m are input and output fuzzy sets, respectively. The ranging error estimation process using the Mamdani FIS model is performed in five steps as follows:

Step 1: Fuzzification step

$$S_{1,a,b} = \mu_{X_a^b}(x_a) \tag{16}$$

where $a = 1, \cdots, n$ and $b = 1, \ldots, i$ are associated with each input. The antecedent MF is a Gaussian function as it gives the best performance among different membership functions [30].

$$\mu_{X_a^b}(x_a) = \exp\left\{-\left(\frac{x_a - \gamma_{ab}}{\vartheta_{ab}}\right)^2\right\} \tag{17}$$

where γ_{ab} and ϑ_{ab} are the parameters referred to as input premise (Gaussian) parameters.

Step 2: Inference or rule step

$$S_{2,i} = \beta_i = \mu_{X_1^i}(x_1) \times \mu_{X_2^i}(x_2) \times \cdots \mu_{X_a^i}(x_a) \tag{18}$$

where $i = 1, \cdots m$. Firing strength β_i of the rule is generated using the product (AND) method [30].

Step 3: Implication step

$$S_{3,i} = \beta_i \circ \mu_{Y^i}\left(y^i\right), \tag{19}$$

where $i = 1, \cdots m$. In this instance, the implication operator (i.e., '$\circ$') is a product. Like antecedent MF, consequent MF ($\mu_{Y^i}\left(y^i\right)$) is also Gaussian function:

$$\mu_{Y^i}\left(y^i\right) = \exp\left\{-\left(\frac{y^i - \alpha_i}{\rho_i}\right)^2\right\}, \tag{20}$$

where α_i and ρ_i are the parameters referred to as output premise (Gaussian) parameters.

Step 4: Aggregation step

$$S_4 = \sum_{i=1}^{m} \beta_i \circ \mu_{Y^i}\left(y^i\right), \tag{21}$$

Step 5: Defuzzification step

$$S_5 = \Delta_e = Z \circ S_4, \tag{22}$$

The crisp output Δ_e is estimated with the defuzzification method (Z) centroid [30].

VI. EXPERIMENTAL EVALUATION

The purpose of the experimental study is twofold. In the first stage, we empirically analyze the measured parameters and compare as well as verify with theoretical analysis of the CIR parameters' uncertainties presented in Section-IV. The analyses are supportive in designing the FIS model parameters and rules. In the second stage, we evaluate the performance of the proposed FIS model in real-time environments. During our measurements, waveforms, estimated distance, channel data, overall received power, and first path received powers for LOS and NLOS conditions are collected in different scenarios and environments as described below.

A. ENVIRONMENTS & SCENARIOS

We collect the measurements in two different environments: Office and a Warehouse. The covered area of the office and the warehouse are 4.88×9.06 and 3.6×8.34-meter square (m^2), respectively. These are located inside the engineering building of the University of Windsor. The characteristics of the two environments are different. In the office, cubical spaces having wooden wall separation, and concrete pillars are utilized to create NLOS scenarios as shown in Fig. 4(a). In each cubical space, a desk, a chair, and a metal cabinet are placed. There are also glass walls that enclose the area and are utilized to create NLOS conditions. In the warehouse, the area is designated as research and development for automobile engines and parts. It has metal pillars. The area is semi-open space with metal parts that mimic an industrial environment as shown in Fig. 4(b).

In both environments, the nodes are placed on trapezoids to collect measurements as shown in Fig. 4. The LOS and NLOS scenarios are created by placing TX and RX nodes at different intervals between 1.92 m and 11.31 m. The NLOS scenarios are emulated using the single wall, multiple walls,

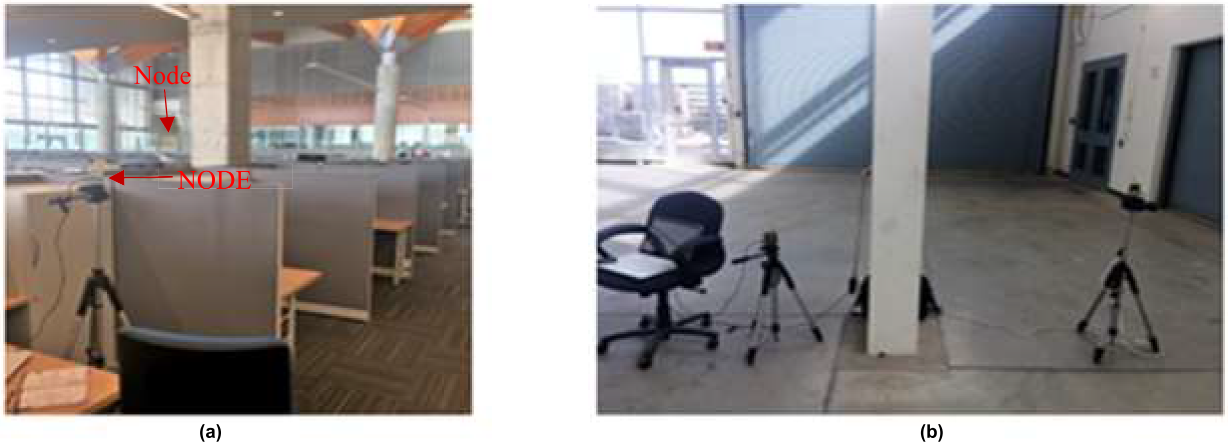

FIGURE 4. Scenarios. (a) Office. (b) Warehouse.

concrete and metal pillars, glass wall, a human body, and different objects such as chairs and metallic parts. In all, there are 30 scenarios where 700 measurements of the parameters are collected.

B. EQUIPMENT SETUP

For the experimental measurements, Decawave® EVB-1000 IR-UWB kit, based on DW-1000, is employed. The kit provides CIRs (or waveforms), range estimations, $RSS_{inst.}$, $FPPS_{inst.}$ and other parameters as outputs from received signal through software. The algorithm used for range estimation in the kit is based on LED-ToA algorithm given in IEEE 802.15.4a framework. During the measurements, Channel 2, having 500MHz bandwidth, 6.8 Mbps data rate and center frequency of 3.5 GHz, is utilized. More details of the kit, operating channels and MAC parameters, and datasheets can be found in [22]. Moreover, Beaglebone® Black Rev. C with A8 ARM cortex processor having 1 GHz clock is employed for code profiling. More details of the board can be found in [31].

C. EMPIRICAL PARAMETERS ANALYSIS

The empirical analysis of the uncertainties in the parameters is supportive in designing the input and output MFs using (15) and (18), respectively as shown in Fig. 5. We analyze the measured parameters (i.e., $RSS_{inst.}$ and $FPPS_{inst}$ levels, RT and ranging errors) based on the theoretical uncertainties analysis of the parameters presented in Section-IV. From the measurements, we observe that for LOS condition in all scenarios, the $RSS_{inst.}$ is in the range of -78 to -80 dBm, while $FPPS_{inst}$ is in the range of -80 to -82 dBm. Therefore, in order to design the MFs and convert the ranges into linguistic variables, the ranges are labeled as very high, as illustrated in Fig. 5. For mild NLOS condition, the $RSS_{inst.}$ is in the range of -80 to -82 dBm, while $FPPS_{inst}$ is in the range of -82 to -86 dBm and labeled as high. Subsequently, as the NLOS severity increases, the $RSS_{inst.}$ and $FPPS_{inst}$ levels consequently attenuate and the ranges are labelled as medium, low, and very low as shown in Fig. 5. Based on the observations, we find that $RSS_{inst.}$ and $FPPS_{inst}$ levels are very high in LOS scenarios and attenuate gradually as the NLOS severity increases. Those observations prove the veracity of the uncertainty model in (3) and (4).

Similarly, we observe that for all the scenarios in LOS condition, the RT is in the range of 3-4 ns. and is labeled as very low. For mild NLOS condition, the RT is in the range of 5-10 ns. and is labeled as low. As the NLOS severity increases, the RT increases, and the ranges are labeled as medium, high, and very high, accordingly, as illustrated in Fig. 5.

For LOS condition, we find that the ranging errors are in the range of -15 to -2 cm: thus, the range is labeled as negative (NE), as shown in Fig. 5. The errors can be negative, as discussed in Case 1 in Section IV. However, for mild NLOS conditions, the ranging errors are in the range of 2 to 12 cm and labeled as very low (V. Low). Moreover, as the severity of the NLOS condition increases, the ranging error magnitude increases and the ranges are labeled as low medium and high, as shown in Fig. 5.

D. MITIGATION PROCEDURE

The proposed FIS model is blindly (i.e., without a priori knowledge of LOS or NLOS condition) applied to the experimentally collected CIR parameters (i.e., $RSS_{inst.}$, $FPPS_{inst}$, and RT) to estimate ranging errors. The inference mechanism estimates the fuzzified ranging error based on the fuzzy inputs. The fuzzified ranging error is defuzzified to determine an estimated crisp value ($\pm\Delta_e$). The Δ_e is subtracted from the reported corresponding measured range to correct the range. The corrected range is called a fuzzy range.

E. PROFILING PROCEDURE

The proposed FIS model, Fuzzy-CIR model [14], and machine learning regression models [18] are implemented in Simulink and run on Beaglebone® Black platform using

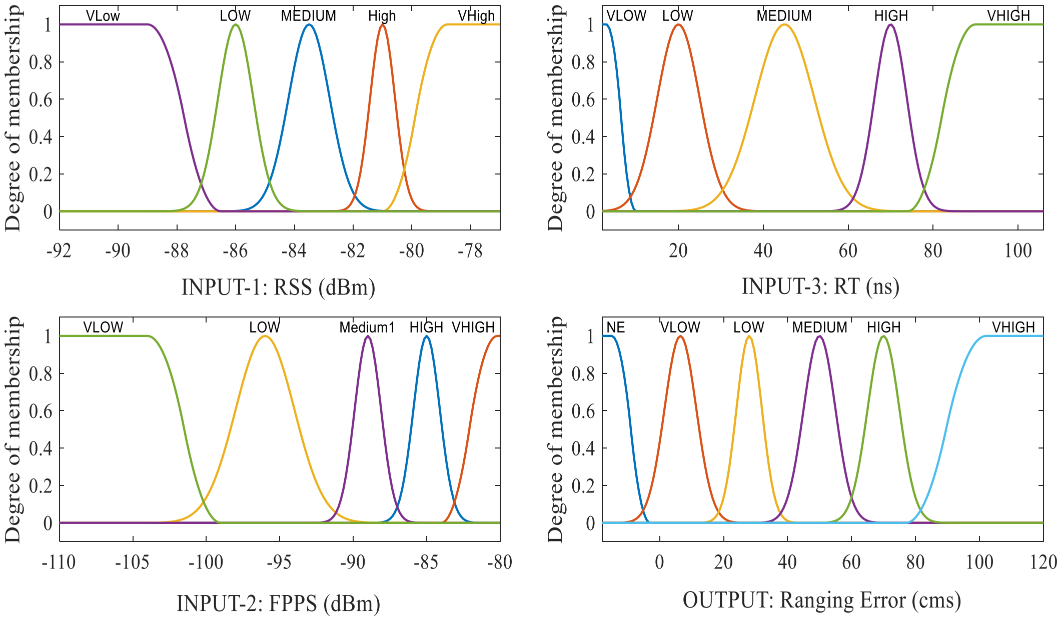

FIGURE 5. Inputs & outputs memberships and linguistic variables for the fuzzy inference system.

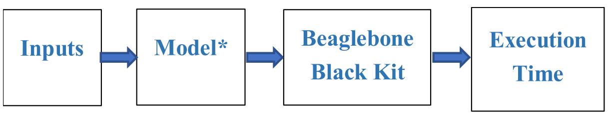

*Fuzzy proposed model / Fuzzy-CIR / Machine-SVM / Machine-GR

FIGURE 6. System block diagram for code profiling.

the processor-in-loop (PIL) procedure for estimating task execution time as shown in Fig. 6. The time is estimated using Monte Carlo simulations for 5000 executions.

F. PERFORMANCE ANALYSIS

The fuzzy mitigation ranging performance is quantified in terms of both the residual ranging errors (ε), (i.e., errors remaining after mitigation), and the root mean square error (RMSE) as shown in Fig. 7 and provided in Table I, respectively. Moreover, a quantitative comparison of computational performance in terms of execution time is provided in Table 1. The RMSE is estimated using the actual error and the predicted error. The figure demonstrates the cumulative distribution function (CDF) of the residual errors for the proposed fuzzy model along with existing works from [14] and [18], and unmitigated LOS and NLOS errors. The proposed model is compared with Fuzzy-CIR model [14], Machine-SVM model [18] and Machine-gaussian regression (GR) model [18]. The parameters used for Fuzzy-CIR are SNR, RMS delay spread, kurtosis, and skewness which are estimated using our experimentally collected CIR data. In Decawave® devices, for the suggested optimum threshold level (δ) [22], ranging errors in LOS conditions are more on the negative side within -10 cm for most of the readings. Moreover, in some experimental setups, in LOS conditions, where the estimated distance is more than 10 m, the ranging

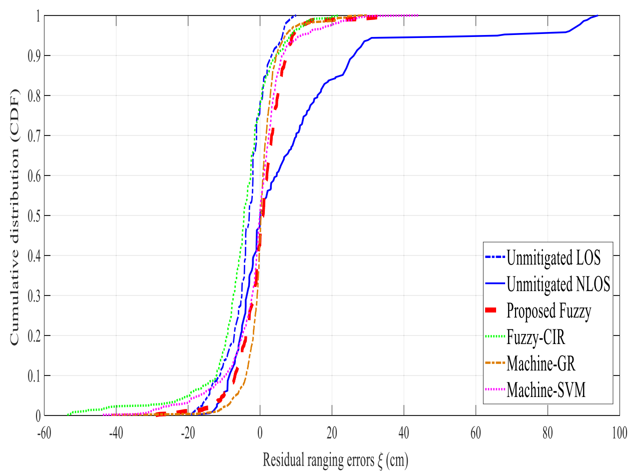

FIGURE 7. Residual ranging errors cumulative distribution function.

TABLE 1. Quantitative comparison between the proposed model and existing works.

Parameters	Proposed Fuzzy	Fuzzy-CIR [14]	Machine-SVM [18]	Machine-GR [18]
Execution time (µs)	1.03	1.09	1.4	640.9
RMSE (cm)	8.1	10.9	8.9	5.1

errors exceed up to -20 cm, as shown in Fig. 7. This is also observed for some soft NLOS (SNLOS) cases in which TX and RX are obstructed and the strongest path is the first path followed by weak MPCs in CIR.

We consider the ranging errors in LOS and SNLOS conditions and estimate ranging errors using the proposed model based on $RSS_{inst.}$, $FPPS_{\text{inst}}$, and RT levels in those conditions. The machine learning based regression models are also

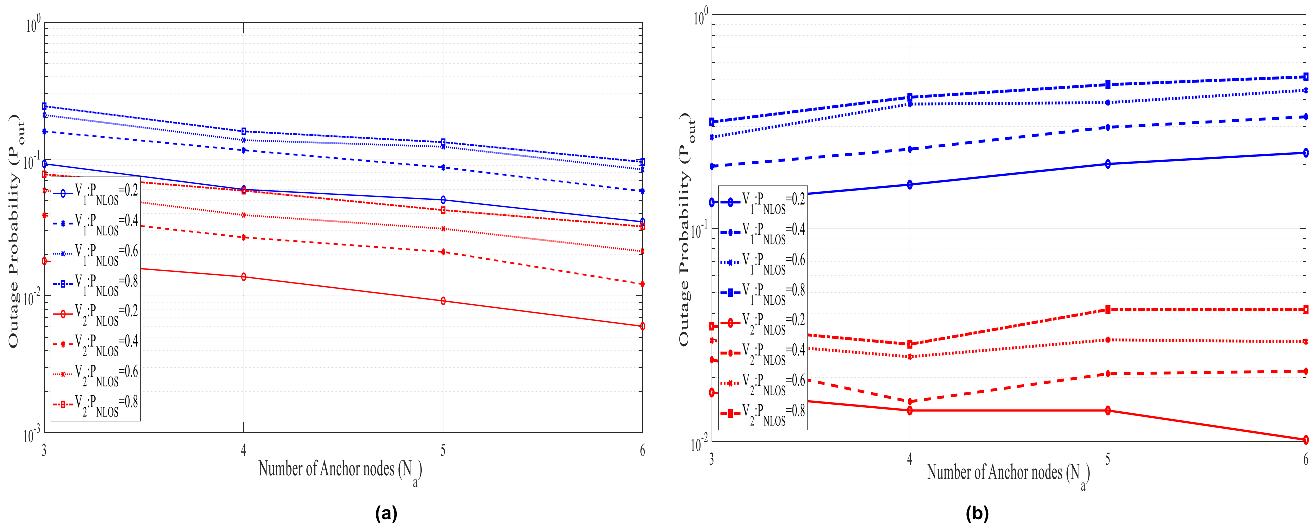

FIGURE 8. Outage probability versus the number of Anchor nodes (N_a) with varying P_{NLOS} in: (a) Warehouse; (b) Office.

trained to predict errors in these conditions using $RSS_{inst.}$, $FPPS_{\text{inst}}$, and RT. However, Fuzzy-CIR does not consider LOS and SNLOS ranging errors. For the proposed fuzzy model, most of the residual errors are confined between upper and lower bounds (i.e., between ± 10 cm) as illustrated in Fig. 7. Moreover, the figure shows an evidence that the errors are confined within the bounds with the estimated CDF of 90.97%. Whereas, in the case of unmitigated NLOS ranging errors in which the estimated CDF is 64.62%. In the case of using the Fuzzy-CIR model, the CDF is 79.87% for ± 10 cm. We observe that the Fuzzy-CIR model's performance, in predicting the errors, decreases in lower ranging errors due to higher estimated RMS delay spread. This phenomena in NLOS conditions occur due to the presence of metal obstructions and ranging errors in the conditions are in the range of 20-40 cm. However, when using the proposed fuzzy model, the uncertainties based on $RSS_{inst.}$, $FPPS_{\text{inst}}$, and RT are optimally covered by the model; hence the error prediction is close to the actual error in the conditions. For higher errors, the performance of both the proposed fuzzy and Fuzzy-CIR models are identical. In comparison with the proposed model, Fuzzy-CIR's RMSE is increased by around 2 cm and the computational time is also increased by around 6%. For Machine-SVM case, we observe that the error prediction performance is identical to the proposed system performance except in some (NLOS) conditions where channel dynamics are changing more often due to high occupancy and the distance between TX and RX is more. Moreover, the Machine-SVM's CDF is 84.5% for the bound. However, the computational time of the Machine-SVM model is increased by approximately 42% comparing to the proposed model. In the case of Machine-GR model, the error prediction performance is better than our proposed model as can be gauged from Machine-GR's estimated CDF of 95.04% and RMSE is of around 5 cm. However, the improvement in error prediction comes at the expense of a huge increase of computational burden as 600 times increase in task execution time comparing to the proposed model.

Therefore, we consider the proposed FIS based mitigated ranges and unmitigated ranges for evaluating the localization performance.

VII. LOCALIZATION PERFORMANCE

The performance of localization is evaluated using fuzzy mitigated ranges and compared with unmitigated ranges. To evaluate the performance, we simulate the localization network using the following settings: ANs $3 \leq N_a \leq 6$ with varying probability of NLOS: $0.2 \leq P_{NLOS} < 1$. The ANs are placed around an agent with the agent's true position $P = (0, 0)$. For every AN $1 \leq i \leq N_a$, the true distance (d_i) is selected from the pool of scenarios associated with the i^{th} scenario and the i^{th} AN's position around the agent is estimated as:

$$A_i = d_i \left(\cos\left(\frac{2\pi\ (i-1)}{N_a}\right), \sin\left(\frac{2\pi\ (i-1)}{N_a}\right)\right) \quad (23)$$

From the ranges' measurements, the estimated distances between the agent and ANs are used to estimate the position of the agent using (1). The i^{th} estimated distance ($\hat{d}_i$) is drawn from NLOS pool with P_{NLOS} and from LOS pool using $(1 - P_{NLOS})$. Likewise, based on the fuzzy mitigated ranges, the estimated agent position is determined using (1), and the i^{th} fuzzy range ($\tilde{d}_i$) associated with the i^{th} scenario is selected for the i^{th} AN.

The reliability of the localization is measured in terms of outage probability (P_{out}). The P_{out} is defined as the probability that the position error is greater than the threshold error and computed as:

$$P_{out}\ (e_{th}) = \left\{ \left\| P - \hat{P} \right\|_2 > e_{th} \right\} \quad (24)$$

where $\hat{P}$ is the estimated position. In this context, we also consider threshold error (i.e., $e_{th} = 15$ cm). The P_{out} is determined using Monte Carlo simulation for 5000 networks implemented using (23) and the target agent for each set of N_a.

The P_{out} for networks with ANs from 3 to 6 with varying P_{NLOS} for both the environments, namely, warehouse and office, are illustrated in Fig. 8. In the figure, the P_{out} using unmitigated ranges and fuzzy mitigated ranges are labelled as V_1 and V_2, respectively. As shown in the figure, the P_{out} is less than 10% with low P_{NLOS} (i.e. 0.2) for both V_1 and V_2. However, as the P_{NLOS} increases, the P_{out} increases. In the case of V_2, P_{out} is relatively low as it is consistently below 10% even for high P_{NLOS} in both the environments. It is also observed that as P_{NLOS} increases, P_{out} does not decrease even with increasing N_a. This is due to high ranging errors in the unmitigated ranges, particularly observed in the office environment as illustrated in Fig. 8(b).

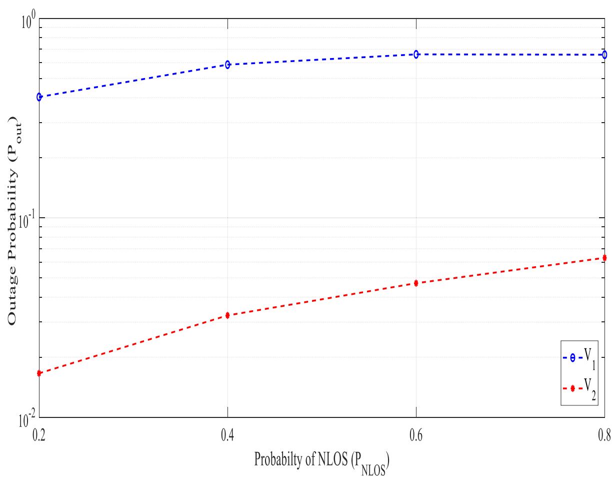

FIGURE 9. **Outage probability versus P_{NLOS} in the worst scenarios with number of anchor nodes ($N_a = 3$).**

Consider $N_a = 3$ for the worst-case scenarios for both the environments, as shown in Fig. 9. The worst-case scenarios are defined as the ranging errors are in the range of 40-100 cm under NLOS conditions. According to the figure, the P_{out} is consistently high for every P_{NLOS} using the unmitigated ranges. However, P_{out} is considerably low as it is consistently less than 10% for the system when using the fuzzy ranges (V_2) compared to V_1. For instance, for equal probability of AN in LOS/NLOS (i.e., $P_{NLOS} = 0.6$), the system's availability is more than 95% (i.e., $1 - P_{out}$) when using the fuzzy mitigated ranges. In contrast, the system's availability reduces to around 66% when using the unmitigated ranges. This is because of a considerable reduction of ranging errors in the case of fuzzy mitigated ranges.

VIII. CONCLUSION

Traditionally, statistical and machine-learned methods are employed to tackle ranging errors and to enhance the accuracy of localization in IR-UWB. However, those methods add a delay in position updates and computational burden in indoor tracking and navigation systems. Moreover, machine learning based models are cumbersome to train and specific to the trained scenarios. In this paper, we have proposed to employ fuzzy logic to estimate the ranging error and to enhance the localization accuracy. In addition, the fuzzy mechanism is employed to cope with the errors present in the LOS conditions due to MPP. The ranging errors are estimated blindly. In other words, prior or posterior knowledge of LOS or NLOS conditions is not required. The ranging correction and the localization performance are evaluated in terms of the CDF of the residual errors, RMSE and the outage probability with extensive experimental measurements in indoor environments using IR-UWB devices. Moreover, computational time is estimated to gauge the computational burden using the targeted embedded system. The experimental results have shown that the residual errors after the fuzzy correction are concentrated around ideal LOS performance, specifically those which have minimal errors. Furthermore, for the proposed model, the attained error convergence for ± 10 cm is improved by 27%, 12%, and 7% compared to the unmitigated NLOS errors, using Fuzzy-CIR scheme and Machine-SVM method, respectively. In addition, the proposed fuzzy model reduces the computational complexity (in terms of execution time) by 42% and around 600 times when compared with Machine-SVM and Machine-GR models, respectively.

Likewise, when using the fuzzy corrected ranges, the simulated localization system has shown more robustness against the position errors and has increased the localization reliability when compared with a system using the unmitigated ranges. In case of system reliability with 15 cm position error threshold, on average, the proposed model has shown system's availability of more than 90% while the system's availability for the model using unmitigated ranges is only about 66%. Finally, the result facts have demonstrated the effectiveness of employing the proposed fuzzy logic model for mitigating the ranging errors while reducing the computational burden in IR-UWB.

REFERENCES

[1] D. Dardari, P. Closas, and D. M. Djuric, "Indoor tracking: Theory, methods, and technologies," *IEEE Trans. Veh. Technol.*, vol. 64, no. 4, pp. 1263–1278, Apr. 2015.

[2] C. Fuchs, N. Aschenbruck, P. Martini, and M. Wieneke, "Indoor tracking for mission critical scenarios: A survey," *Pervasive Mobile Comput.*, vol. 7, pp. 1–15, Feb. 2011.

[3] M. M. Atia, S. Liu, H. Nematallah, T. B. Karamat, and A. Noureldin, "Integrated indoor navigation system for ground vehicles with automatic 3-D alignment and position initialization," *IEEE Trans. Veh. Technol.*, vol. 64, no. 4, pp. 1279–1292, Apr. 2015.

[4] J. Park, Y. K. Cho, and D. Martinez, "A BIM and UWB integrated mobile robot navigation system for indoor position tracking applications," *J. Construct. Eng. Project Manage.*, vol. 6, no. 2, pp. 30–39, 2016.

[5] A. Vale, R. Ventura, P. Lopes, and I. Ribeiro, "Assessment of navigation technologies for automated guided vehicle in nuclear fusion facilities," *Robot. Auto. Syst.*, vol. 97, pp. 153–170, Nov. 2017.

[6] M. Zhou, Y. Wei, Z. Tian, X. Yang, and L. Li, "Achieving cost-efficient indoor fingerprint localization on WLAN platform: A hypothetical test approach," *IEEE Access*, vol. 5, pp. 15865–15874, 2017.

[7] Q. Li, W. Li, W. Sun, J. Li, and Z. Liu, "Fingerprint and assistant nodes based Wi-Fi localization in complex indoor environment," *IEEE Access*, vol. 4, pp. 2993–3004, 2016.
[8] L. Luoh, "ZigBee-based intelligent indoor positioning system soft computing," *Soft Comput.*, vol. 18, pp. 443–456, Mar. 2014.
[9] Z. Daixian and Y. Kechu, "Particle filter localization in underground mines using UWB ranging," presented at the Intell. Comput. Technol. Automat. (ICICTA), 2011. [Online]. Available: https://ieeexplore.ieee.org/abstract/document/5750971/citations#citations
[10] Y. Xu, Y. S. Shmaliy, Y. Li, and X. Chen, "UWB-based indoor human localization with time-delayed data using EFIR filtering," *IEEE Access*, vol. 5, pp. 16676–16683, 2017.
[11] B. Silva and G. P. Hancke, "IR-UWB-based non-line-of-sight identification in harsh environments: Principles and challenges," *IEEE Trans. Ind. Informat.*, vol. 12, no. 3, pp. 1188–1195, Jun. 2016.
[12] V.-H. Nguyen and J.-Y. Pyun, "Location detection and tracking of moving targets by a 2D IR-UWB radar system," *Sensors*, vol. 15, no. 3, pp. 6740–6762, 2015.
[13] D. Dardari, A. Conti, U. Ferner, A. Giorgetti, and M. Z. Win, "Ranging with ultrawide bandwidth signals in multipath environments," *Proc. IEEE*, vol. 97, no. 2, pp. 404–426, Feb. 2009.
[14] K. Wen, K. Yu, and Y. Li, "NLOS identification and compensation for UWB ranging based on obstruction classification," presented at the 25th Eur. Signal Process. Conf. (EUSIPCO), 2017. [Online]. Available: https://ieeexplore.ieee.org/abstract/ document/8081702
[15] S. Yousefi, X. W. Chang, and B. Champagne, "An improved extended Kalman filter for localization of a mobile node with NLOS anchors," presented at the 9th Int. Conf. Wireless Mobile Commun., 2013. [Online]. Available: http://www.ece.mcgill.ca/~bchamp/Papers/Conference/ICWMC2013b.pdf
[16] I. Güvenç *et al.*, "NLOS identification and weighted least-squares localization for UWB systems using multipath channel statistics," *EURASIP J. Adv. Signal Process.*, vol. 2008, pp. 1–14, Dec. 2007.
[17] S. Marano *et al.*, "NLOS identification and mitigation for localization based on UWB experimental data," *IEEE J. Sel. Areas Commun.*, vol. 28, no. 7, pp. 1026–1035, Sep. 2010.
[18] H. Wymeersch, S. Maranó, W. M. Gifford, and M. Z. Win, "A machine learning approach to ranging error mitigation for UWB localization," *IEEE Trans. Commun.*, vol. 60, no. 6, pp. 1719–1728, Jun. 2012.
[19] S. Tian, L. Zhao, and G. Li, "A support vector data description approach to NLOS identification in UWB positioning," *Math. Problems Eng.*, vol. 2014, May 2014, Art. no. 963418.
[20] M. Kolakowski and J. Modelski, "First path component power based NLOS mitigation in UWB positioning system," presented at the Telecommun. Forum (TELFOR), 2017. [Online]. Available: https://ieeexplore.ieee.org/abstract/document/8249313
[21] B. You, X. Li, X. Zhao, and Y. Gao, "A novel robust algorithm attenuating non-line-of-sight errors in indoor localization," presented at the IEEE Int. Conf. Commun. Softw. Netw. (ICCSN), 2015. [Online]. Available: https://ieeexplore.ieee.org/abstract/document/7296117
[22] *Decawave*. [Online]. Available: www.decawave.com
[23] Y.-H. Wang, C.-H. Yeh, H.-W. V. Young, K. Hu, and M.-T. Lo, "On the computational complexity of the empirical mode decomposition algorithm," *Phys. A, Stat. Mech. Appl.*, vol. 400, pp. 159–167, Apr. 2014.
[24] T. Velmurugan and T. Santhanam, "Computational complexity between K-means and K-medoids clustering algorithms for normal and uniform distributions of data points," *J. Comput. Sci.*, vol. 6, no. 3, pp. 363–368, 2014.
[25] P. Melin and O. Castillo, "A review on type-2 fuzzy logic applications in clustering, classification and pattern recognition," *Appl. Soft Comput.*, vol. 21, pp. 568–577, Aug. 2014.
[26] P. Torteeka and X. Chundi, "Indoor positioning based on Wi-Fi fingerprint technique using fuzzy K-nearest neighbor," presented at the 11th Int. Bhurban Conf. Appl. Sci. Technol. (IBCAST), 2014. [Online]. Available: https://ieeexplore.ieee.org/abstract/document/6778188
[27] S. K. Meghani and M. Asif, "Localization of WSN node based on RTT ToA using ultra wide band & 802.15.4a channel," presented at the IEEE 11th Int. Conf. Netw., Sens. Control (ICNSC), 2014. [Online]. Available: https://ieeexplore.ieee.org/abstract/document/6819656
[28] Y. Touati, R. Merzouki, and B. O. Bouamama, "Robust diagnosis to measurement uncertainties using bond graph approach: Application to intelligent autonomous vehicle," *Mechatronics*, vol. 22, pp. 1148–1160, Dec. 2012.
[29] H. Mazar, "The main radio regulated services," in *Radio Spectrum Management: Policies, Regulations and Techniques*, 1st ed. Hoboken, NJ, USA: Wiley, 2016. [Online]. Available: https://books.google.ca/books?hl=en&lr=&id=ysqOCQAAQBAJ&oifnd&pg=PA13&dq=Radio+Spectrum+Management:+Policies,+Regulations+and+Techniques&ots=6aC9WNWxHS&sig=smjAvg29847J2VCo6rTwzAVMZmg#v=onepage&q=Radio%20Spectrum%20Management%3A%20Policies%2C%20Regulations%20and%20Techniques&f=false
[30] A. Celikyilmaz and I. B. Türksen, *"Modeling Uncertainty with Fuzzy Logic With Recent Theory and Applications"* (Studies in Fuzziness and Soft Computing). Springer, vol. 240. 2009, pp. 149–215. [Online]. Available: https://link.springer.com/book/10.1007%2F978-3-540-89924-2
[31] *Beaglebone Black*. [Online]. Available: https://beagleboard.org/black

SUNIL K. MEGHANI received the B.S. degree in electronic engineering from the Sir Syed University of Engineering and Technology, Karachi, Pakistan, in 2002, the M.Sc. degree in modern digital radio frequency and wireless communication from the University of Leeds, Leeds, U.K., in 2007, and the Ph.D. degree in electrical engineering from the University of Windsor, Canada, in 2018. He was a Network Engineer with Electro International Pakistan, from 2003 to 2005. From 2008 to 2014, he was with the Sir Syed University of Engineering and Technology, Pakistan, as an Assistant Professor. From 2014 to 2018, he was a Research Assistant and a Ph.D. candidate with the Wireless Communication and Information Processing (WiCIP) Lab, University of Windsor, Canada, where he is currently a Research Associate. His current research interests are focused on autonomous vehicles, indoor localization, wireless sensor networks (WSN), fuzzy logic and machine learning-based classifiers, IR-UWB, and wireless personal area networks (WPAN).

MUHAMMAD ASIF received the B.S. degree in biomedical engineering from the Sir Syed University of Engineering and Technology, Karachi, Pakistan, in 2002, the M.S. degree in electrical engineering from University Sains Malaysia (USM), Malaysia, in 2007, and the Ph.D. degree in electrical engineering from the National University of Sciences and Technology (NUST), Karachi, in 2015. In USM, he was with the USM Robotics Research Group on various underwater robotics and vision systems. After completing his M.S. degree from USM Malaysia, he is currently pursuing the Ph.D. degree with NUST. During his Ph.D., he worked on robotics and control engineering. He has organized and participated in various robotics competitions on national and international levels like ROBOCON, ROBOCOM, and NERC. He has more than 45 research publications in international and national journals and conferences. His research interests include fuzzy systems, adaptive and nonlinear control and vision algorithms design for robotics, and vision applications; moreover, embedded systems design for medical and the IoT applications.

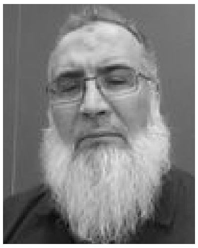

FAROQ AWIN received the B.Sc. degree in electrical and electronic engineering from the University of Tripoli, Libya, in 1996, the M.Sc. degree in precision instruments and machinery from Beihang University, Beijing, China, in 2004, and the Ph.D. degree from the University of Windsor, Canada, in 2016. He was a Researcher with the Electronic Research Center, Tripoli, Libya, from 1997 to 2008. From 2008 to 2010, he was a Lecturer with the Electrical and Electrical Engineering Department, University of Tripoli. From 2011 to 2016, he was a Research Assistant and a Ph.D. candidate with the University of Windsor, where he is currently a Post-Doctoral Fellow with the Wireless Communication and Information Processing (WiCIP) Laboratory. He has published several articles in well-known journals and international conferences. His research interests include cognitive radio networks, spectrum sensing, wireless communications, cognitive radio-based IoT and indoor tracking. Moreover, he is serving as a Peer Reviewer for a couple of referred international journal and conferences.

KEMAL TEPE received the M.A.Sc. and Ph.D. degrees from the Rensselaer Polytechnic Institute, Troy, NY, USA, in 1996 and 2001, respectively, and the B.Sc. degree from Hacettepe University, Ankara, Turkey, in 1992, all in the electrical engineering. He worked as a Research Scientist with Telcordia Technologies, Red Bank, NJ, USA, and a Postdoctoral Researcher with Rutgers University, from 2001 to 2002. He joined the University of Windsor, in 2002, and has founded the Wireless Communication and Information Processing Research Laboratory. His research area focuses on wireless communication systems, vehicle-to-vehicle (V2V) communications, wireless sensor networking, and network protocols. He is particularly interested in real-time wireless communication protocols in sensor networks, application of sensor networking in smart grid applications, vehicular networks, vehicular networks for safety/emergency messaging, vehicular internet access protocols, the Internet of Things (IoT), autonomous vehicles, and machine-to-machine communications.